

Anisotropy in Second-Harmonic Generation from Reconstructed Surfaces of GaAs

Chikashi Yamada and Takahiro Kimura

Optoelectronics Technology Research Laboratory, 5-5 Tohkodai, Tsukuba, Ibaraki, 300-26, Japan

(Received 16 November 1992)

We report on the first observation of the twofold rotational anisotropy of second-harmonic generation (SHG) in the reflected light from a noncentrosymmetric crystal surface of GaAs(001). We interpret this as meaning that the interference of surface SHG and dipole-allowed bulk SHG having fourfold symmetry results in twofold anisotropy. The degree of anisotropy changes according to the surface reconstruction.

PACS numbers: 78.66.Fd, 42.65.Ky, 68.35.Rh

Optical second-harmonic generation (SHG) in reflection from surfaces has been proven to be a useful tool for studying both surfaces and interfaces. So far, however, its applications have been limited mostly to centrosymmetric materials, such as Si, to name one which has attracted much interest in semiconductor studies [1]. The reason is that in centrosymmetric materials SHG is forbidden in bulk (as long as the electric dipole approximation holds) and, therefore, any SHG signal is considered to originate from surfaces. (As recent experiments and theory show, the bulk quadrupolar contribution to surface reflection SHG can no longer be neglected [1] in the cases where the bulk dipolar component is missing.)

On the other hand, in noncentrosymmetric materials, such as GaAs, dipole-allowed bulk SHG can be quite intense and, thus, hampers surface observations. Stehlin *et al.* [2] have discussed the optical ray geometry relative to the crystal axes in which only the surface component of SHG can be observed. They used SHG as a surface probe to observe the adsorption of tin on a GaAs(001) surface. Buhaenko *et al.* [3] observed a large SH intensity variation during the adsorption of trimethylgallium on a GaAs(001) surface under conditions in which a substantial bulk contribution would have been expected. In our recent paper [4] we described the SH intensity change during photochemical washing as well as sulfur passivation processes of a GaAs(001) surface in a liquid environment, in which the surface-specific component was selected by choosing the P_{in} - P_{out} configuration at a rotation angle of 0° . At the present stage, there has been no intensive study carried out concerning the rotational anisotropy of the SH intensity from a GaAs surface. In this Letter we report on the first observation of the rotational anisotropy of surface reflection SHG from GaAs(001). We also found that the efficiency of surface SHG and therefore the degree of anisotropy change according to the surface reconstruction.

Figure 1 shows the experimental setup. A vacuum chamber with a base pressure of 2×10^{-8} Pa was used, in which the electron beam of a RHEED (reflection high-energy electron diffraction) apparatus was aligned in the plane of light incidence in order to determine the sample rotation angle and to observe the RHEED pattern. A

dye laser provided linearly polarized light pulses of about 10 ns duration with an energy of 10–15 mJ and a 30 Hz repetition rate. The wavelength of the laser light was set to 580 nm throughout the experiment. We guided the laser pulse so that it illuminated the sample at an incident angle of 60° after passing through a polarizer and a lens of $f=50$ cm. The sample was mounted on a rotation stage having a sample heating capability. The fluence of the laser pulses was limited to ~ 10 mJ/cm² in order to avoid any damage due to transient heating and/or electronic-excitation-induced defect formation. The reflected SH light was detected by a solar-blind photomultiplier coupled with an analyzer and long-wavelength cut filters. The signal from the photomultiplier was fed to a gated integrator to obtain an average signal over 100 shots.

The GaAs sample was grown homoepitaxially on an *n*-type GaAs substrate, (001) faced ($\pm 0.03^\circ$), with our molecular-beam-epitaxy (MBE) facility. Soon after crystal growth a clear 2×4 diffraction pattern was observed by RHEED. Subsequently, the sample was passivated by cooling it to below 0°C under the ambient arsenic pressure in the same MBE chamber [5]. After maintaining the temperature below 0°C for several hours the sample was allowed to reach room temperature. The

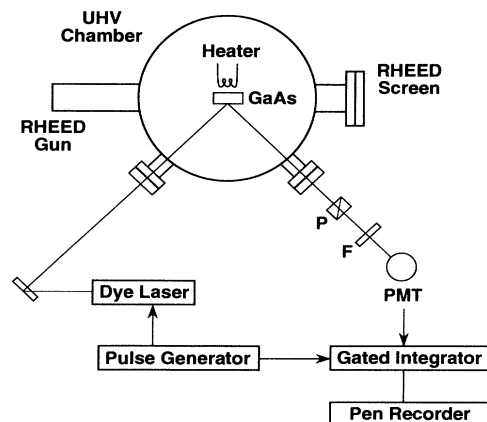


FIG. 1. Experimental arrangement.

sample was then transferred through air to the SHG measurement chamber.

In the SHG measurement chamber the arsenic passivating cap layer on the GaAs surface was removed by heating the sample to 350°C for several minutes. After the sample was further heated to 460°C and then cooled to room temperature, a twofold streak pattern was observed by RHEED for the electron beam incident on the [110] azimuth, accompanied by fourfold vague lines between them. For the $\bar{1}\bar{1}0$ azimuth, we observed widely separated streaks corresponding to the fundamental period of the reciprocal lattice. The RHEED pattern of this “2×1” reconstruction is shown in Fig. 2(a). For this surface, anisotropy was observed in the SHG intensity, as shown in Fig. 4(a). This figure clearly shows a twofold symmetry; i.e., every other peak of the four is stronger than the others. We observed this in an optical-ray geometry having P_{in} - P_{out} configuration, as shown in Fig. 3, in which the rotation angle was also defined, i.e., 0° for the [100] direction.

The same sample was then again heated to 630°C, where the RHEED pattern showed changes from 2×1 to 4×2. As soon as the pattern changed to 4×2 the sample was allowed to cool down to room temperature. RHEED showed a streaky fourfold pattern accompanied by weak threefold lines between them as well as a sixfold streak pattern for electron beams incident on the [110] and $\bar{1}\bar{1}0$ azimuths, respectively [Fig. 2(b)]. SHG was measured on this “4×6” surface in the same configuration as that for the 2×1 surface. The SHG intensity also showed

twofold symmetry with four peaks and four valleys; the intensity difference between the higher peaks at $\varphi=135^\circ$ and 315° and the weaker peaks at $\varphi=45^\circ$ and 225° was more prominent than for the 2×1 surface. On the other hand, in the S_{in} - P_{out} configuration we observed a fourfold symmetry within the experimental uncertainty, although the peak height was about one-fifth of the stronger peak of the P_{in} - P_{out} configuration.

A phenomenological theory has been developed for cubic centrosymmetric semiconductors, such as Si, by Sipe, Moss, and van Driel [6]. For semiconductors with a zinc-blende structure, such as GaAs, we extend Sipe’s theory by adding a tensor element of bulk susceptibility, $\partial_{36}=\partial_{xyz}$ (the only nonzero element for zinc-blende type crystal [7]). At the same time we must allow the effective symmetry of the surface to lower from C_{4v} to C_{2v} , corresponding to the observed symmetry of the rotation angle dependence. The 2×1 and 4×2 reconstructions, the latter being one of the two constituents of the 4×6 surface, have C_{2v} symmetry, but the 2×6, the other component, lacks C_{2v} symmetry (C_1) [8]. It should also be noted that a misoriented surface would lower the overall symmetry to C_s [9–11]. However, within the experimental error of the present experiment, we did not observe any lower symmetry in the rotational angle dependence, meaning that tensor elements appearing only in the C_s symmetry or lower are negligibly small. Further, we notice that the mirror planes for the C_{2v} reconstructed surface are rotated from the x axis by 45° about the surface normal. We define the ξ and η axes as being the principal axes for the surface tensor elements, e.g., $\partial_{15}=\partial_{\xi\xi\eta}$, etc., as shown in Fig. 3. Sticking to the definition of angle $\varphi=0$ being on the x axis, the $\cos(2\varphi)$ terms in Sipe’s result must be replaced by $\sin(2\varphi)$ and $\cos(4\varphi)$ must be $-\cos(4\varphi)$; we also change $x \rightarrow \xi$ and $y \rightarrow \eta$ for those terms with surface tensor components. We then obtained the following expression for the harmonic electric field in P_{in} - P_{out} configuration:

$$E_{pp}^{(2\omega)}/E_p^2 A_p = a_{pp} + (c_{pp}^{(2)} + d_{pp}^{(2)}) \sin(2\varphi) - c_{pp}^{(4)} \cos(4\varphi), \tag{1}$$

where a , $c^{(2)}$, and $c^{(4)}$ are coefficients which have already been defined in the paper of Sipe, Moss, and van Driel

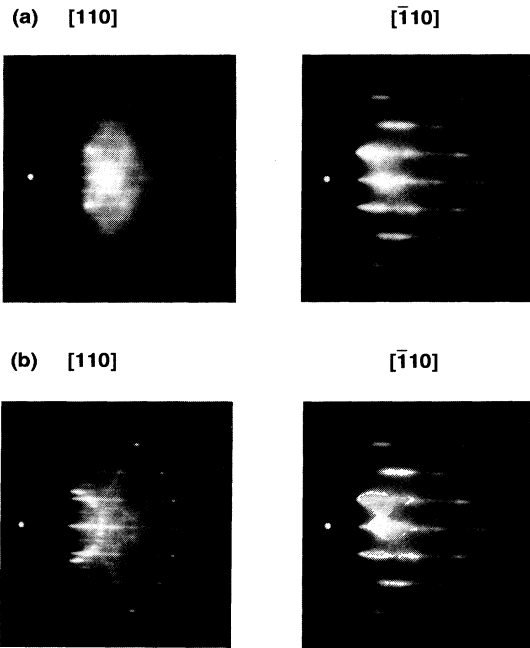


FIG. 2. RHEED pattern of the 2×1 surface (a) and 4×6 surface (b).

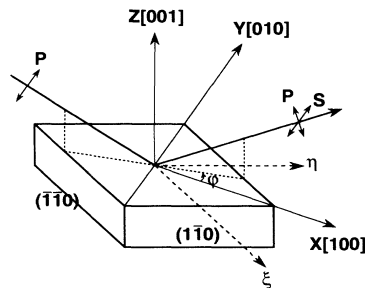


FIG. 3. Optical ray geometry relative to the crystal axes.

(here we have rewritten the suffix \parallel, \parallel as pp); $d_{pp}^{(2)}$ represents the bulk dipole contribution introduced for a non-centrosymmetric crystal,

$$d_{pp}^{(2)} = \partial_{xyz} \left(\frac{1}{2} F_s f_c^2 - F_c f_c f_s \right). \quad (2)$$

Note that the a and c coefficients (complex numbers) contain contributions from the bulk electric quadrupole, the bulk magnetic dipole, as well as the surface dipole terms. A similar expression for the S_{in} - P_{out} case is derived as

$$E_{sp}^{(2\omega)}/E_s^2 A_p = a_{sp} + (c_{sp}^{(2)} + d_{sp}^{(2)}) \sin(2\varphi) + c_{sp}^{(4)} \cos(4\varphi), \quad (3)$$

where

$$d_{sp}^{(2)} = -\frac{1}{2} \partial_{xyz} F_s. \quad (4)$$

In this case the a_{sp} term (isotropic term) contains only the bulk quadrupolar and the surface dipolar terms with the $\partial_{z\xi\xi} + \partial_{z\eta\eta}$ components, and no terms with ∂_{zzz} or $\partial_{\xi\xi z} + \partial_{\eta\eta z}$ which are present in the P_{in} - P_{out} case. The $c^{(2)}$ terms appearing in both Eqs. (1) and (3) comprise the anisotropic part of the quadrupolar and surface dipolar terms, i.e., $\partial_{z\xi\xi} - \partial_{z\eta\eta}$ and $\partial_{\xi\xi z} - \partial_{\eta\eta z}$ in $c_{pp}^{(2)}$, and $\partial_{z\xi\xi} - \partial_{z\eta\eta}$ in $c_{sp}^{(2)}$. The $c^{(4)}$ terms contain only the electric quadrupole contribution.

Although a rigorous separation of these contributions is impossible, we can reasonably state that the bulk quadrupolar and magnetic dipolar contributions are negligible compared to the bulk dipolar terms since they are about $(a/\lambda)^2$ times smaller than the electric dipole contribution, where a is the representative size of an atom and λ is the wavelength [12].

The anisotropic surface dipolar term, $\partial_{z\xi\xi} - \partial_{z\eta\eta}$, cannot be determined independently, because it has the same rotation angle dependence as that of the stronger bulk term, ∂_{xyz} , either in P_{in} - P_{out} or S_{in} - P_{out} configuration (see Table I). Another anisotropic surface dipole term $\partial_{\xi\xi z} - \partial_{\eta\eta z}$ is also indeterminate either in P_{in} - P_{out} or P_{in} - S_{out} configuration. The isotropic term $\partial_{z\xi\xi} + \partial_{z\eta\eta}$ is con-

sidered to be small because we observed in the S_{in} - P_{out} configuration a fourfold symmetry corresponding to the squared sine term,

$$I \propto |(c^{(2)} + d^{(2)}) \sin(2\varphi)|^2. \quad (5)$$

Notice that the addition of a constant term to the sine term results in a twofold symmetry.

Consequently, the remaining surface dipolar terms which need consideration are ∂_{zzz} and $\partial_{\xi\xi z} + \partial_{\eta\eta z}$, and they give an isotropic rotation-angle dependence in the P_{in} - P_{out} configuration. Therefore, the observed rotation-angle dependence can be written as

$$I(\varphi) = |A + B \sin(2\varphi)|^2, \quad (6)$$

where A represents the isotropic surface contribution and B contains bulk dipole and (small) surface anisotropic terms. We least-squares fitted the observed rotation-angle dependence for both the 2×1 and 4×6 data by Eq. (6) with A and B used as adjustable parameters. We obtained, as a measure of the isotropic surface contribution, a ratio of $A/B = -0.013$ for the 2×1 surface and $A/B = -0.037$ for the 4×6 surface. As shown in Fig. 4, the fit was satisfactory. Since bulk (dipolar) SHG is forbidden at angles of 0° , 90° , 180° , and 270° , the surface SHG is the only component. However, as can be seen in Fig. 4, the difference in the intensity for the 2×1 and 4×6 surfaces is hard to recognize at these angles, since the SHG intensity is below the experimental error limit. Here, we notice, however, that instead of directly looking at the SH intensities at these angles we can observe a difference in the surface condition (reconstruction) through only a change in the degree of anisotropy. That is, any small change in the surface-specific (isotropic) SHG component is amplified to the apparent anisotropy.

TABLE I. Rotation-angle dependences of the second-order susceptibility tensor components for C_{2v} symmetry. Only the dipolar (surface and bulk) terms are listed. See Ref. [6] for the coefficients to be multiplied to these tensor components.

| Polarization | Isotropic a term | $\sin(2\varphi)$ $c^{(2)}, d^{(2)}$ terms | $\cos(2\varphi)$ |
|----------------------|--|--|---|
| P_{in} - P_{out} | $\partial_{z\xi\xi} + \partial_{z\eta\eta}$ $\partial_{\xi\xi z} + \partial_{\eta\eta z}$ ∂_{zzz} | $\partial_{z\xi\xi} - \partial_{z\eta\eta}$ $\partial_{\xi\xi z} - \partial_{\eta\eta z}$ ∂_{xyz} | ... |
| S_{in} - P_{out} | $\partial_{z\xi\xi} + \partial_{z\eta\eta}$ | $\partial_{z\xi\xi} - \partial_{z\eta\eta}$ ∂_{xyz} | ... |
| P_{in} - S_{out} | ... | ... | $\partial_{\xi\xi z} - \partial_{\eta\eta z}$ ∂_{xyz} |
| S_{in} - S_{out} | ... | ... | ... |

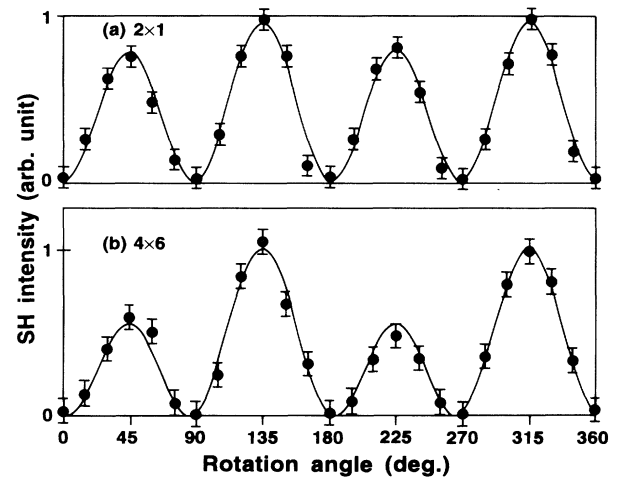


FIG. 4. Observed rotational anisotropy of the SH intensities in the reflected light from (a) GaAs(001) 2×1 and (b) GaAs(001) 4×6 surfaces. The solid lines indicate the calculated rotation-angle dependence [Eq. (6)].

It is interesting that Kamiya *et al.* [13] observed anisotropies in the linear reflectance-difference (RD) signal from GaAs (001) surfaces. They assigned, for example, in the 4×2 reconstructed surface, a broad peak at a photon energy of 1.9 eV (in which our 580 nm wavelength is included) to the bonding to the lone-pair state transition of the Ga dimers on the surface. They used near normal incidence *S*-polarized input light so that the RD spectrum is inherently sensitive to optical transitions whose transition moment is parallel to the (001) face. It is also quite probable in our case that the resonance effect due to the Ga dimer through the term with $\partial_{\xi\xi z} + \partial_{\eta\eta z}$ enhanced the surface SHG, since in the 4×6 reconstruction Ga dimers exist and in the 2×1 reconstruction they do not [8,14].

Another point we should like to point out is that atomic transitions of Ga, $4d^1D \leftarrow 4p^1P^\circ$ and $4d^1P^\circ \leftarrow 4p^1P^\circ$, lie at 294.3 and 287.4 nm, respectively [15], which are near the SH light wavelength (4.28 eV). If this near resonance is preserved for the surface bonded Ga atoms [16], it might contribute to the isotropic ∂_{zzz} element.

The advantage of using visible light as an input beam, as opposed to the usual cases of using 1.06 mm laser light, must be noted. Because of shorter penetration depths of fundamental as well as the second-harmonic lights, which can be shorter than the coherence lengths [17], the relative magnitude of the bulk SHG becomes smaller, if the surface contribution stays constant.

In conclusion, we have observed the twofold anisotropy in the rotation-angle dependence of the SH intensity in $P_{in}\text{-}P_{out}$ configuration, and assigned it to an interference effect of the fourfold bulk term and the constant surface dipole term. It is interesting to note that C_{2v} surface symmetry could explain our result, although the 4×6 surface contains domains with C_s symmetry. We noticed, however, that for the 4×6 surface in the $S_{in}\text{-}S_{out}$ configuration (where the bulk contribution is zero), there exists nonzero SHG, meaning the existence of symmetry which is lower than C_{2v} . However, its rotation-angle dependence was difficult to measure, because the signal was so poor. Apparently, an improvement of the sensitivity will be the next progress, and we are making efforts on this line.

The authors' appreciation goes to Akihiro Hashimoto

and Tohru Saito for the help in preparing the As-passivated samples. The authors also thank Yoshifumi Katayama for his critical reading of the manuscript.

-
- [1] For a recent review, T. F. Heinz, in *Nonlinear Surface Phenomena*, edited by H. E. Ponath and G. I. Stegeman (North-Holland, Amsterdam, Netherlands, 1991).
 - [2] T. Stehlin, M. Feller, P. Guyot-Sionnest, and Y. R. Shen, *Opt. Lett.* **13**, 389 (1988).
 - [3] D. S. Buhaenko, S. M. Francis, P. A. Goulding, and M. E. Pemble, *J. Cryst. Growth* **97**, 595 (1989).
 - [4] C. Yamada, T. Kimura, and P. Fuqua, *Jpn. J. Appl. Phys.* (to be published).
 - [5] S. Kowalczyk, D. L. Miller, J. R. Waldrop, P. G. Newman, and R. W. Grant, *J. Vac. Sci. Technol.* **19**, 255 (1981).
 - [6] J. E. Sipe, D. J. Moss, and H. M. van Driel, *Phys. Rev. B* **35**, 1129 (1987).
 - [7] See, for example, P. N. Butcher and D. Cotter, *The Elements of Nonlinear Optics* (Cambridge Univ. Press, Cambridge, 1990).
 - [8] D. K. Biegelsen, R. D. Bringans, J. E. Northrup, and L.-E. Swartz, *Phys. Rev. B* **41**, 5701 (1990).
 - [9] C. W. van Hasselt, M. A. Verheijen, and Th. Rasing, *Phys. Rev. B* **42**, 9263 (1990).
 - [10] M. A. Verheijen, C. W. van Hasselt, and Th. Rasing, *Surf. Sci.* **251**, 467 (1991).
 - [11] R. W. J. Hollering and M. Barmantlo, *Opt. Commun.* **88**, 141 (1992).
 - [12] V. B. Berestetsky, E. M. Lifshits, and L. P. Pitaevsky, *Relativistic Quantum Theory* (Nauka, Moscow, 1968), Pt. 1, Secs. 49,50.
 - [13] I. Kamiya, D. E. Aspnes, H. Tanaka, L. T. Florez, J. P. Harbison, and R. Bhat, *Phys. Rev. Lett.* **68**, 627 (1992); D. E. Aspnes, Y. C. Chang, A. A. Studna, L. T. Florez, H. H. Farrell, and J. P. Harbison, *Phys. Rev. Lett.* **64**, 192 (1990).
 - [14] D. J. Chadi, *J. Vac. Sci. Technol. A* **5**, 834 (1987).
 - [15] C. E. Moore, *Atomic Energy Levels* (National Bureau of Standards, Washington D.C., 1949).
 - [16] N. Kobayashi and Y. Horikoshi, *Jpn. J. Appl. Phys.* **30**, L1443 (1991).
 - [17] R. K. Chang and N. Bloembergen, *Phys. Rev.* **144**, 775 (1966).

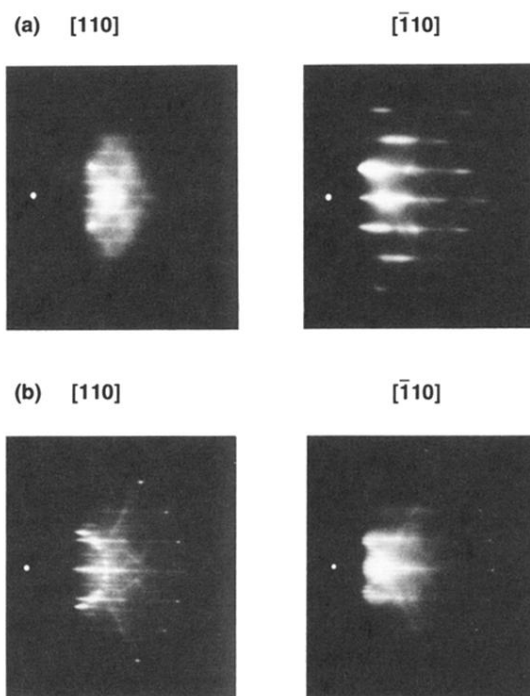


FIG. 2. RHEED pattern of the 2×1 surface (a) and 4×6 surface (b).